A statistical tensile model of fibre reinforced cementitious composites

Y. WANG, S. BACKER and V. C. LI

(Massachusetts Institute of Technology, USA)

A statistical model has been developed to predict the tensile constitutive relationship of FRC from fibre and matrix properties and geometries. This tensile relation for FRC is also used to predict the load–deformation relations for the compact tension test and the flexural test configurations. Theoretical load–deformation relations of FRC were compared with results from these tests and good qualitative agreement was obtained for different FRC. There still exists a difference between the magnitudes of the theoretical and the experimental data. Possible sources of this discrepancy are discussed as a basis for ongoing theoretical and experimental studies aimed at reducing this discrepancy.

Key words: *fibre reinforced concrete; mathematical model; tensile properties; compact tension test; flexural test; synthetic fibre*

NOMENCLATURE

a	Crack length of compact tension specimen (CTS)
b	Slippage distance of fibre end
B	Thickness of CTS, or width of beam
CV_{lc}	Coefficient of variation of L_c
d_f	Fibre diameter
E_f	Elastic modulus of the fibre
E_m	Elastic modulus of the matrix
f_c	Beam deflection at mid-span
H	Net width of CTS, or height of beam
l	Fibre embedded length
L	Specimen length
L_c	Fibre critical length of pull-out
L_f	Fibre staple length
M	Bending moment in beam
N	Number of fibres bridging the crack
N_0	Number of fibres originally bridging the crack
N_t	Number of fibres located within a distance of $L_f/2$ from the crack plane
P	Force of CTS
$p(y)$	Probabilistic density function of variable y
q	Displacement of CTS
V_f	Fibre volume fraction
w	Crack opening width
x	Fibre stretched length
$\bar{x}$	Average stretched length for all bridging fibres
x_m	Maximum stretched length among all fibres
z	Distance between fibre centroid and the crack plane
α	Fraction ratio of load-carrying fibres
β	Normalized location of neutral plane in CTS or beam
σ_c	Mean stress of the composite
σ_f	Fibre stress at exit point from matrix
$\overline{\sigma_f}$	Average fibre stress for all bridging fibres
σ_f^u	Ultimate strength of fibre
τ	Fibre matrix bond shear stress
δ	Specimen elastic deformation
Δ	Fibre elastic elongation
ϕ	Fibre orientation angle relative to the normal of crack
ε_c	Composite strain
ε_m^u	Matrix cracking strain
ε_t	Maximum tensile strain in beam

Being a material which is inexpensive, readily available, durable, and easily formed into required structures, concrete is heavily used in civil engineering constructions. However, its poor behaviour in tension is a serious drawback which limits its use in many applications.

Fibre reinforcement has been proven to be an effective and economical way to improve the properties of concrete, even with just a few volume percent of fibres in the concrete matrix. Asbestos cement has been successfully used in factory- prefabricated elements for nearly a century,[1] and was extensively used all over the

0010-4361/89/030265-10 $3.00

world. Recently its use has been generally banned in many countries for health reasons. Research has been carried out in the past two decades on fibre reinforced cementitious composites (FRC) using other fibres such as steel, glass, synthetic and natural fibres, and great progress has been made. The application area of FRC has also been widely expanded.

One of the major advantages of fibrous composites is that the composite properties can be controlled, within a certain range, by varying the governing parameters, which include the properties and geometries of the reinforcing fibres and the matrix. Due to the technological sophistication of the synthetic fibre industry which has made available a wide range of fibres with varieties of properties and geometry, there is an increased chance to obtain the fibres needed to produce desired materials. However, in order to determine the requirements for reinforcing fibres and to optimize FRC design, it is still necessary to find the relationships which relate FRC properties to the parameters of its structural components. Further, constitutive equations relating material deformations to applied loads are a prerequisite for establishing the bases for design of FRC structures. Such relationships are certainly needed for the linear elastic region of material behaviour. Of equal, if not greater importance, is an understanding of the mechanisms of FRC resistance to cracking and to crack propagation.

Toward this understanding, numerous theories of FRC have been developed.[2–5] Most theories to date deal with the cracking and ultimate strengths of FRC. Recently Ganeshalingham, Paramasivam and Nathan[6] evaluated a number of the existing theories of FRC behaviour in tension and in flexure, comparing cracking and ultimate stresses obtained from theory with results of experiments. Less work has been reported on details of load–displacement relations after cracking is initiated, and this has been the focus of this study.

The constitutive modelling of the tensile behaviour of FRC leads to a description of deformation before and after matrix first cracking in terms of fibre and matrix parameters. It has been suggested[7] that the best way to describe the crack resistance of FRC, whose improvement is the greatest contribution of the fibre, is by means of a tension–crack separation curve. This paper first presents a statistical model of FRC under uniaxial tension. The tensile constitutive relation for FRC is then applied to two test configurations readily subjected to laboratory confirmation: the compact tension test and the flexural test. Results and comparison with experimental data are then discussed.

TENSILE STRESS–STRAIN RELATION OF FRC

Concrete reinforced with discrete fibres randomly distributed in the matrix is investigated in this study. Prior to loading, it is not possible to determine the location and geometry of the first matrix crack, nor the distribution of fibres bridging the crack. This indicates the statistical nature of FRC behaviour.

To describe the FRC tensile behaviour after matrix cracking, a single fibre being pulled out from a matrix is considered, and its pulling force and the accompanying deformation are related to the fibre/matrix geometry and properties. The probabilistic density functions of embedded fibre lengths and fibre orientations relative to the crack plane are then established. These probabilistic density functions, together with the geometric compatibility condition, permit the calculation of the mean stress of the composite for each strain from the relation found in the simple pull-out problem.

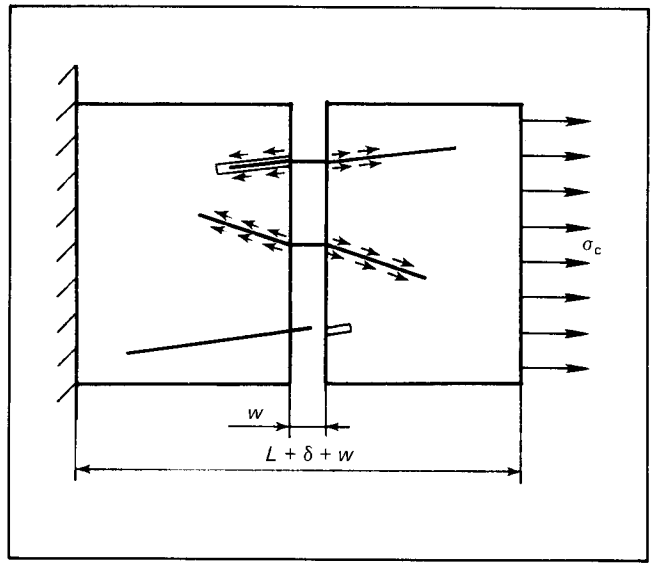

Fig. 1 Schematic diagram of an FRC specimen under uniaxial tension

Problem statement and assumptions

Consider an FRC specimen under a static, uniaxial tension test, as illustrated in Fig. 1, which is monotonically stretched to failure. In order to find the stress–strain relation, as recorded by a stiff test machine, a few assumptions are made:

1) Fibres in the matrix are in 3-dimensional random distribution, straight, separated, and all with the same circular cylindrical geometry
2) Both fibre and the matrix are linear elastic up to failure.
3) The bond between fibre and matrix is purely frictional and constant along the fibre length, therefore the shear resistance of the fibre/matrix bond has a constant value, τ.
4) Fibres are completely flexible so that the bending effect at the fibre exit point from the cracked matrix is neglected; similarly the concentrated (snubbing) friction force at the fibre exit point is neglected.
5) Only one plane crack perpendicular to the load will be developed, since randomly distributed fibre reinforced concrete generally fails in a single fracture mode.

Fibre pull-out problem

Consider a fibre with an embedded length l in a matrix, being stretched by a force (Fig. 2). At low stress levels, the fibre segment inside the matrix is only stretched

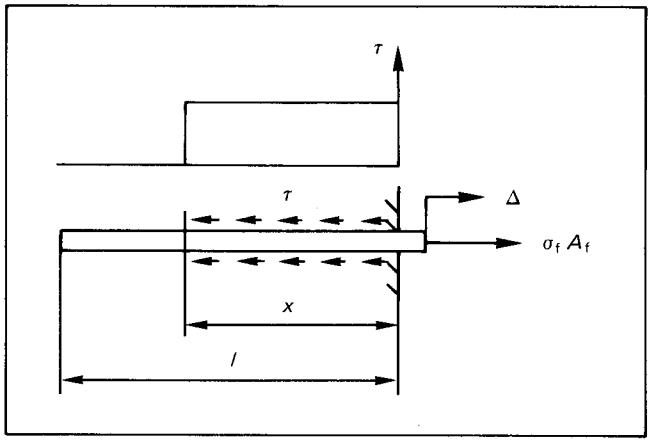

Fig. 2 A fibre being pulled out from a matrix

along a length x, which is related to the pulling stress σ_f by:

$$\sigma_f = \frac{4\tau x}{d_f} \tag{1}$$

and the fibre elastic elongation Δ is given by:

$$\Delta = \int_0^x \frac{\sigma_f(x)}{E_f}\,dx = \frac{2\tau x^2}{E_f d_f} \tag{2}$$

Equations (1) and (2) imply that the fibre segment of length x slips relative to the matrix as it stretches.

As the external stress (σ_f) increase, the stretched length (x) will also increase, according to Equation (1), until x reaches l, the embedded fibre length, at which moment the fibre becomes fully stretched and the fibre end begins to slip. Then the fibre stretched length (x) decreases according to:

$$x = l - b \tag{3}$$

where b is the slippage distance of the fibre end.

It is also possible that the fibre stress (σ_f) reaches the ultimate strength of the fibre (σ_f^u) first, and the fibre breaks before it is stretched to its end. The critical length of pull out, L_c, which is defined as the maximum embedded length for a fibre to be pulled out rather than broken, can be found from:

$$L_c = \frac{d_f \sigma_f^u}{4\tau} \tag{4}$$

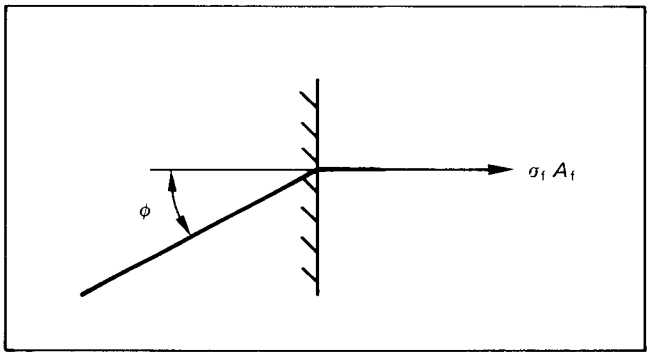

Fig. 3 A fibre being pulled out at an angle ϕ

For a fibre embedded at an angle ϕ to the normal of the matrix surface (Fig. 3), the σ_f–x relation given by Equation (1) and the Δ–x relation of Equation (2) remain valid, since the fibre is assumed to have negligible bending rigidity, and the concentrated (snubbing) friction force at the fibre exit is neglected.

Composite stress–strain relation before matrix cracking

For strains in the FRC composite (ε_c) smaller than the matrix cracking strain (ε_m^u), according to the Law of Mixtures:

$$\sigma_c = kV_f E_f \varepsilon_c + (1 - V_f) E_m \varepsilon_c \qquad \text{for } \varepsilon_c \leq \epsilon_m^u \tag{5}$$

where k is a constant ($k < 1$) which accounts for fibre orientation and unevenness of fibre loading along fibre axes.

Usually for FRC, only low fibre volume fractions are used (V_f = 1–4%), therefore the first term in Equation (5) can be neglected if the fibre elastic modulus is not more than an order of magnitude higher than the matrix modulus.

Composite deformation after matrix cracking

Referring to Fig. 1, it is seen that the deformation of the FRC specimen consists of basically two parts: the crack opening (w), and the elastic deformation of the specimen (δ). Composite strain is related to w and δ by:

$$\varepsilon_c = \frac{\delta + w}{L} \tag{6}$$

The elastic strain (ε/L) can be calculated from the Law of Mixtures, similar to Equation (5), after the composite stress (σ_c) corresponding to w is determined from the stresses of fibres bridging the crack.

Compatibility of fibre deformation at the crack

At a given composite strain level, the fibres originally bridging the crack may include fibres that have been pulled out from that side of matrix with shorter embedded lengths, fibres that have been stressed to rupture, fibres that are partially stretched, and fibres that have been fully stretched whose ends are slipping relative to the matrix. At the crack, the following equation must be satisfied by each fibre which still bridges the crack at the instant when crack opening equals w:

$$2\Delta + \left(1 + \frac{\sigma_f}{E_f}\right) b = w \tag{7}$$

where 2Δ represents the total elastic deformation of the fibre segments embedded in both sides of the crack, σ_f is the fibre stress at the exit point from the matrix, b is the slippage distance of the end of the shorter embedded fibre segment (b = 0 for partially stretched fibres), and $b\sigma_f/E_f$ is the elastic deformation of the fibre segment which has slipped out from the matrix as a result of the end slippage, b.

Relation between fibre stresses and composite stress

After matrix cracking, the total force carried by the composite is equal to the sum of the forces in the fibres bridging the crack:

$$A_c\sigma_c = \Sigma\,(A_f\sigma_f) = N A_f\overline{\sigma_f}$$

or

$$\sigma_c = \alpha\frac{N_0 A_f}{A_c}\overline{\sigma_f} \tag{8}$$

where A_c is the total area of the specimen cross section, A_f is the cross sectional area of the fibre, N is the number of fibres currently bridging the crack, N_0 is the number of fibres originally bridging the crack, $\overline{\sigma_f}$ is the average fibre stress for fibres currently bridging the crack, and $\alpha \equiv N/N_0$, is the fraction ratio of load-carrying fibres. Note that α decreases from 1 to 0 due to fibre pull out and breakage as the crack opening increases.

The expected number of fibres bridging the crack at (and before) matrix cracking (N_0) is determined from the fibre volume fraction (V_f) and distributions of fibre location and orientation. Fibres whose centroids are located at a distance of $L_f/2$ or less from the crack plane (on either side) may intercept the crack plane. The total number of such fibres, N_t, is related to the fibre volume fraction in a straightforward manner:

$$N_t = \frac{A_c L_f V_f}{L_f A_f} = \frac{A_c}{A_f}V_f \tag{9}$$

The distance of the fibre centroid from the crack plane for these fibres, z, is uniformly distributed from 0 to $L_f/2$, with a constant probabilistic density, following the assumption of random fibre placement in the matrix:

$$p(z) = \frac{2}{L_f} \qquad \text{for } 0 \le z \le L_f/2 \tag{10}$$

A fibre whose centroid is at a distance z ($z \le L_f$) from the crack plane will intercept the crack if:

$$\frac{L_f\cos\phi}{2} \ge z$$

or

$$\phi \le \arccos\frac{2z}{L_f} \tag{11}$$

Therefore the probability for a fibre with $z \le L_f/2$ to intercept the crack plane can be evaluated from:

$$\int_{z=0}^{L_f/2}\left[\int_{\phi=0}^{\arccos(2z/L_f)} p(\phi)d\phi\right]p(z)\mathrm{d}z \tag{12}$$

Since fibres are randomly oriented with uniform distribution over the hemisphere, the distribution of the fibre orientation (ϕ) can be obtained as shown in Fig. 4. Using $p(\phi)$ and $p(z)$ given in Fig. 4 and Equation (10), the expression in Equation (12) is determined to be 0.5. Multiplying the total number of fibres which may intercept the crack plane with the probability of their actually intercepting the plane, one obtains the number of fibres originally bridging the crack (N_0):

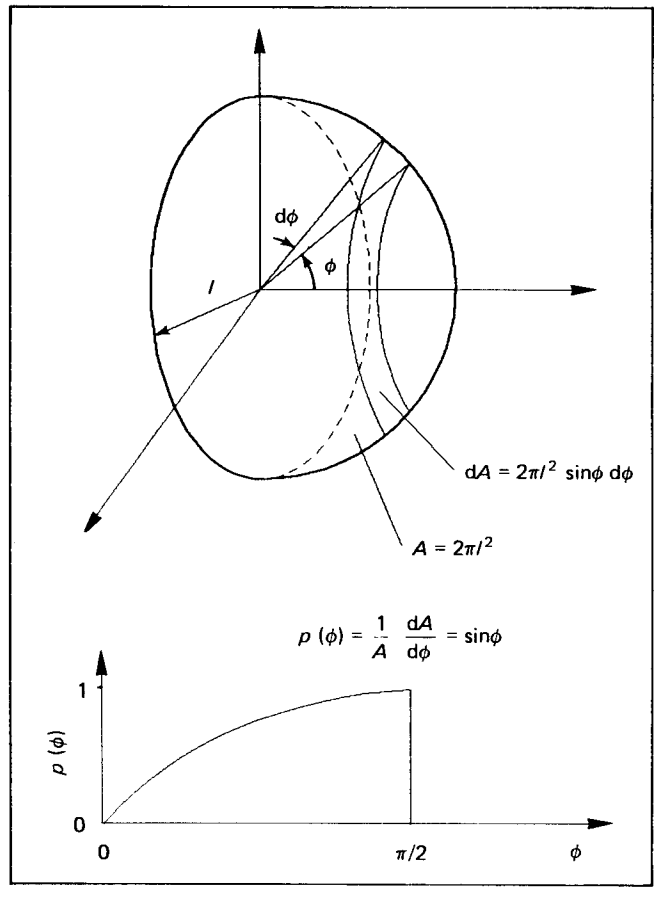

Fig. 4 Fibre angle distribution and its determination. A is the surface area of the hemisphere with a radius l

$$N_0 = 0.5N_t = \frac{V_f A_c}{2A_f} \tag{13}$$

Finally, substituting Equation (13) into Equation (8):

$$\sigma_c = 0.5\alpha V_f\overline{\sigma_f} \tag{14}$$

σ_c–ε_c relation after matrix cracking

So far basic relations have been established for the simple fibre pull-out problem, for deformations of fibres and of composite, and the relation between fibre stress and composite stress. Composite stress corresponding to any composite strain can be readily calculated from Equation (6) once the relation between the crack opening (w) and the composite stress (σ_c) is found. Since the composite stress (σ_c) is directly related to the average fibre stress ($\overline{\sigma_f}$) and the fraction ratio (α) by Equation (14), the next step is to determine $\overline{\sigma_f}$ and α from w.

For a particular fibre bridging the crack, its stress (σ_f) can be calculated from Equation (1):

$$\sigma_f = \frac{4\tau x}{d_f}$$

Therefore the average fibre stress ($\overline{\sigma_f}$) is given by:

$$\overline{\sigma_f} = \frac{4\tau \bar{x}}{d_f} \tag{15}$$

where $\bar{x}$ is the average stretched length for fibres bridging the crack.

The average stretched length of fibres ($\bar{x}$) and the fraction ratio (α) depend on the distribution of fibre embedded length just at matrix cracking, as well as on the distribution of fibre stretched length. At different loading stages, the fractions of fibres at the crack in the categories of broken, pulled out, partially stretched, and fully stretched fibres are different, and the distribution of fibre stretched length (x) changes accordingly. From the distribution of fibre stretched length, $\bar{x}$ and α can be calculated and then the composite stress. The crack opening width (w) can also be obtained from this distribution by the compatibility equation, Equation (7).

Consider the case when $L_f \leq 2L_c$ as an example. Since the maximum possible embedded fibre length relative to the crack is $L_f/2$, it is seen from the definition of fibre critical length (L_c) in Equation (4) that no fibre breakage will take place and all fibres bridging the crack will be eventually pulled out.

At the instant of matrix cracking, the distribution of embedded fibre length is considered to be uniform over the range of 0 to $L_f/2$, as shown in Fig. 5. The maximum length considered is $L_f/2$ since a fibre will be pulled out from the side of matrix with shorter embedded length. At an early loading stage before all the fibres have been fully stretched, the portion of pulled out fibres can be idenfitied as Area I in Fig. 6. For partially stretched fibres, from the compatibility condition, Equation (7) and the Δ–x relation, equation (2), these fibres are all stretched to the same length x_m, to be referred to as the maximum stretched length, which is related to w by:

$$w = 2\Delta = 2\frac{2\tau x_m^2}{E_f d_f} \tag{16}$$

These fibres are represented by Area III in Fig. 6. The rest of the fibres which are fully stretched correspond to Area II in Fig. 6 and their stretched length is just $x = l - b$ (Equation (3)).

From Fig. 6, the fraction ratio of load-carrying fibres (α) is easily calculated:

$$\alpha = 1.0 - \text{Area I} = 1 - w\frac{2}{L_f} \tag{17}$$

After eliminating the pulled out fibres and adjusting for the fibre segments which have slipped out from the matrix, the probabilistic density function for the 'current embedded length', $(l - b)$, can be obtained as shown in Fig. 7, from which the average fibre stretched length ($\bar{x}$) is determined:

$$\bar{x} = \int_{-\infty}^{+\infty} x\,p(x)\,dx = \frac{x_m}{\alpha L_f}(L_f - x_m - w) \tag{18}$$

Similarly, α and $\bar{x}$ can be calculated for loading stages after all the fibres have been fully stretched.

From the above relations, the complete stress–strain relationship for the FRC composite specimen can be calculated as a function of fibre modulus (E_f), fibre length (L_f), fibre diameter (d_f), fibre/matrix bond strength (τ), fibre volume fraction (V_f), matrix modulus (E_m), matrix cracking strain (ε_m^u), and the specimen length (L).

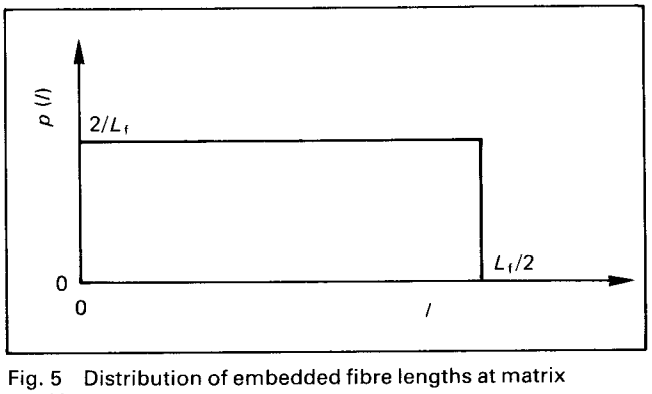

Fig. 5 Distribution of embedded fibre lengths at matrix cracking

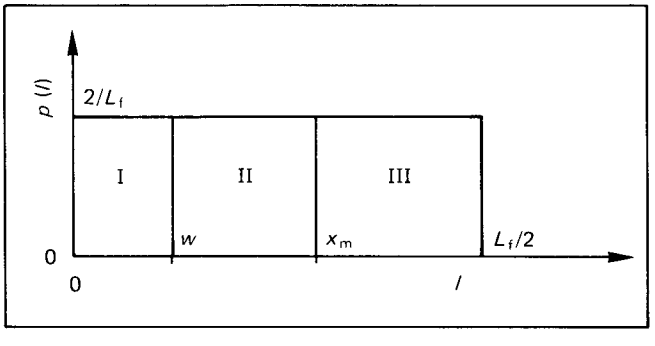

Fig. 6 Portions of fibres under different conditions

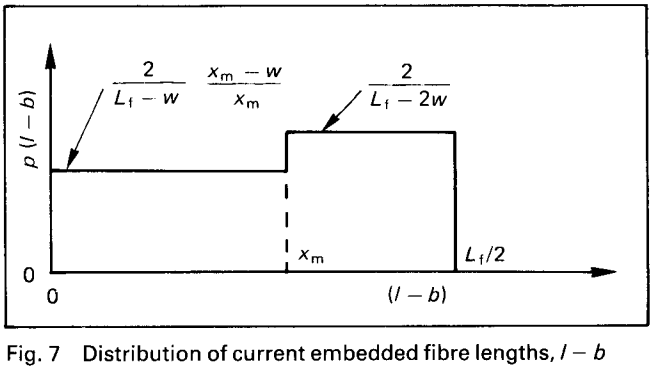

Fig. 7 Distribution of current embedded fibre lengths, $l - b$

For the case when $L_f > 2L_c$, part of fibres originally bridging the crack will be stretched to rupture and others will be pulled out. The probabilistic density function for the stretched fibre length (x) can also be established following similar procedures as done above, with additional consideration of the portion of broken fibres at each instant. The exact forms of the probabilistic density functions can be found elsewhere.[8] In this case, the composite stress–strain relationship is not only dependent on E_f, L_f, d_f, τ, V_f, E_m, ε_m^u, and L, but also dependent on the fibre critical length of pull out (L_c) and its variation (CV_{lc}).

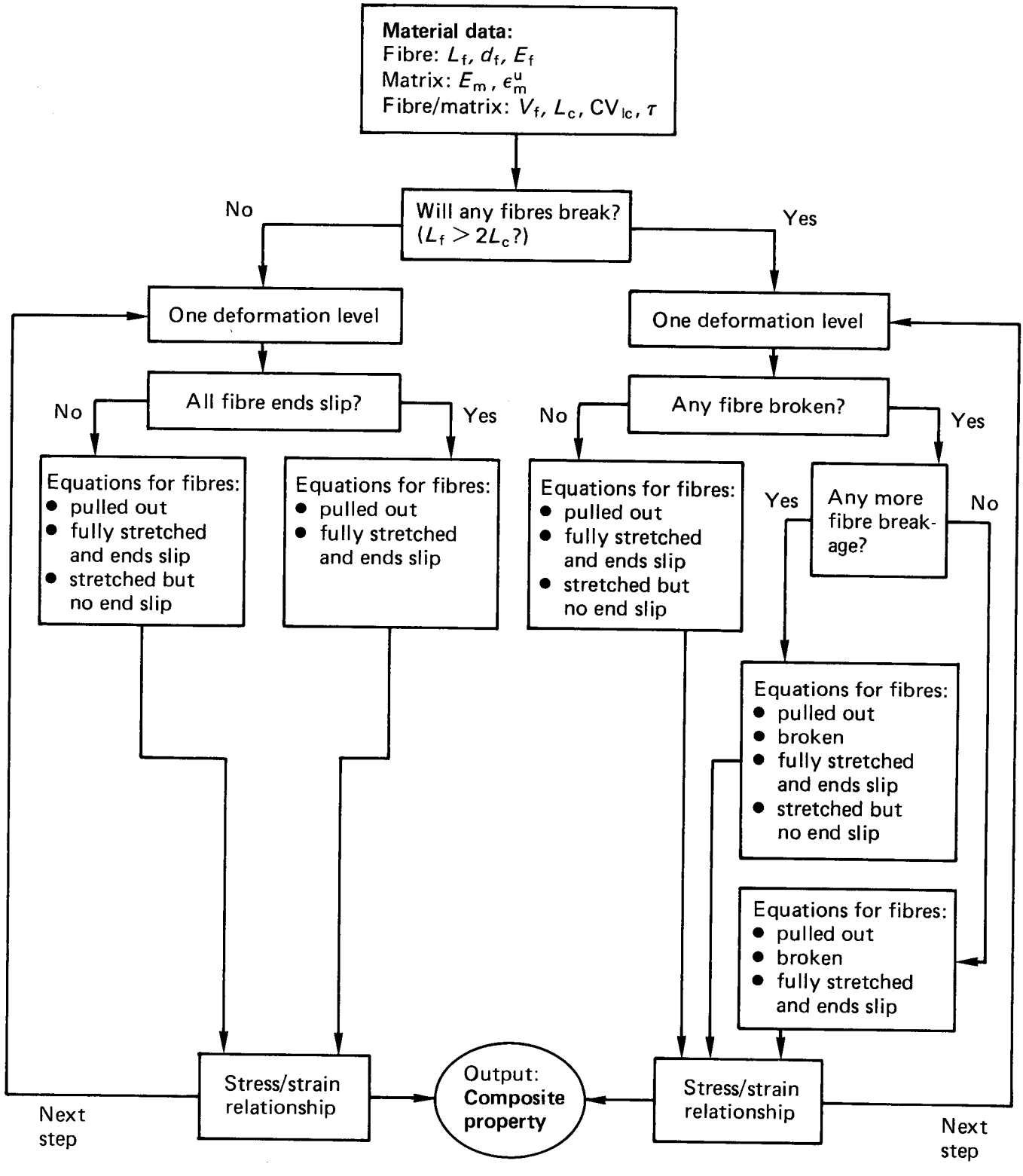

Fig. 8 Flow chart for the tensile model

A computational procedure has been established, the flow chart of which is shown in Fig. 8. The complete composite stress–strain relation is calculated based on measured quantities: E_f, L_f, d_f, τ, V_f, E_m, ε_m^u, L, L_c, and CV_{lc}. The measurement of τ and L_c for certain fibres may require special techniques as used in this study. Further details may be found in Refs 9 and 10.

Fig. 9 shows two theoretical σ_c–ε_c curves for nylon and acrylic reinforcements. Based on experimental measurements,[9] E_f = 5 GPa, σ_f^u = 0.6 GPa, and τ = 2.93 MPa were used for the acrylic fibre, and E_f = 5 GPa, σ_f^u = 1 GPa, and τ = 0.16 MPa for the nylon fibre. CV_{lc} = 0.2 was assumed for the acrylic fibre. Since the nylon fibre considered were expected to be pulled out rather than to rupture, CV_{lc} was not required in this case. In all the calculations, E_m = 10 GPa and ε_m^u = 0.06% were assumed. Fibre dimensions (d_f, L_f) as well as fibre volume fractions (V_f) are indicated in the figure.

As seen from Fig. 9, the the σ_c–ε_c curve is initially linear up to the point when the matrix cracks, at which moment there is a load drop. The magnitude of load drop and the σ_c–ε_c relation beyond matrix cracking are strongly dependent on the reinforcing fibres. The distinctive features between nylon and acrylic FRC reflect the differences between these fibres: acrylic fibre has a high fibre/matrix bond strength (τ) and low strength (σ_f^u), therefore a short critical length of pull out (L_c), while nylon fibre has low τ, high σ_f^u, therefore long L_c, for fibres with similar diameters (d_f). It is thus expected that nylon fibres bridging the crack are more likely to be pulled out rather than broken, resulting in high energy absorption. But shortly after matrix cracking the nylon fibres cannot pick up the load immediately; therefore a significant load drop can be seen at $\varepsilon_c = \varepsilon_m^u$. On the other hand, acrylic fibres bridging the crack are more likely to fail by rupture and they may provide relatively high load shortly after matrix cracking with less or no load drop at $\varepsilon_c = \varepsilon_m^u$.

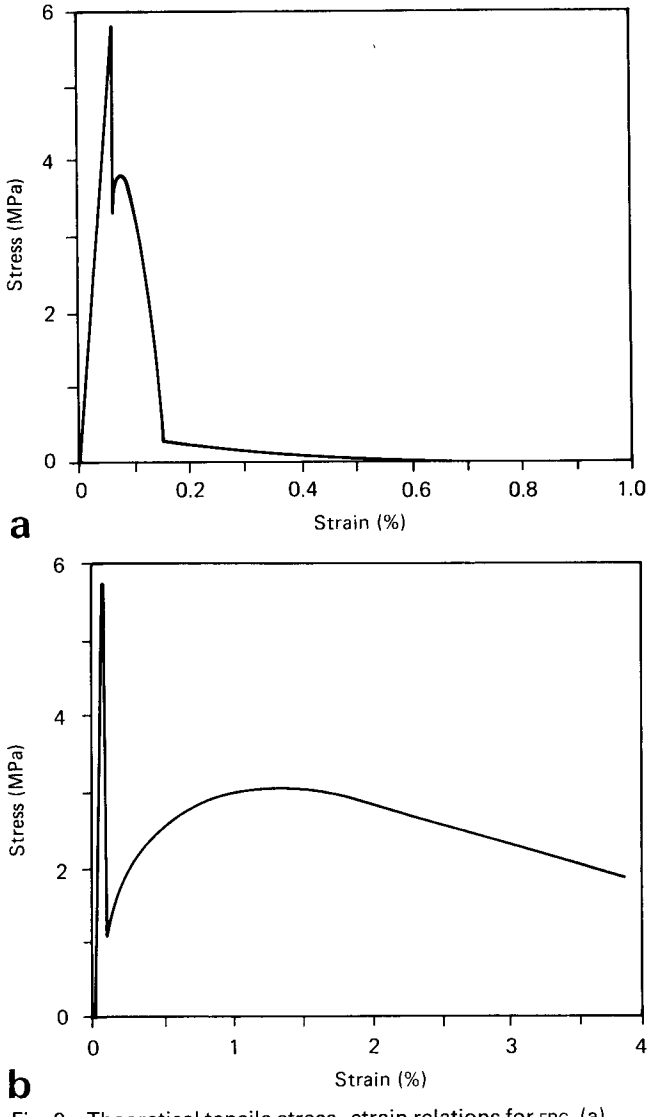

Fig. 9 Theoretical tensile stress–strain relations for FRC. (a) Acrylic FRC: V_f = 2%, L_f = 19.1 mm, d_f = 0.0192 mm, and L = 150 mm; (b) nylon FRC: V_f = 2%, L_f = 38.1 mm, d_f = 0.0176 mm, and L = 150 mm

EXPERIMENTAL VERIFICATION BY COMPACT TENSION AND FLEXURAL TESTS

The most logical way to verify the tensile constitutive model would be by means of a direct uniaxial tension test, which also provides the most useful information on FRC behaviour. However, because of the difficulties in conducting uniaxial tension tests for which special fixtures with high stiffness are required to ensure testing conditions and uniform specimen tensile strains, uniaxial tension tests on FRC specimens were not performed at this time. At this stage of the preliminary study, two tests, the compact tension specimen (CTS) test and the four point flexural test, were used instead to study the properties of FRC and to verify the theoretical predictions of the tensile model. These tests are simple, less test condition dependent, require lower loading capacity, and are frequently used.

In order to make comparisons between the theoretical and the experimental results, relationships are needed to relate the uniaxial tensile constitutive relation to the load–displacement relation for the CTS test and to the moment–curvature relation for the flexual test. A rigorous solution would require a numerical analysis applying the tensile constitutive relation to each local element in solving the equilibrium and geometric compatibililty equations, like that reported by Li and Liang[7] in their analysis of centre-cracked panels. To avoid the complexity in such calculations, two simple models were established to predict the 'test curves' for the CTS and flexural tests, based on assumed forms of strain fields in the specimens. Because of such imposed constraints on the strain fields, the results from these models can only be compared with experimental results qualitatively.

CTS model

Consider a CTS specimen shown in Fig. 10. A linear strain field in the specimen is assumed which is related to the specimen displacement (q) as illustrated by Fig. 11. The linear elastic region of the tensile constitutive relation derived in the previous section (Equation (5)) is considered to apply to the compressive region as well, which is justifiable since the compressive strength

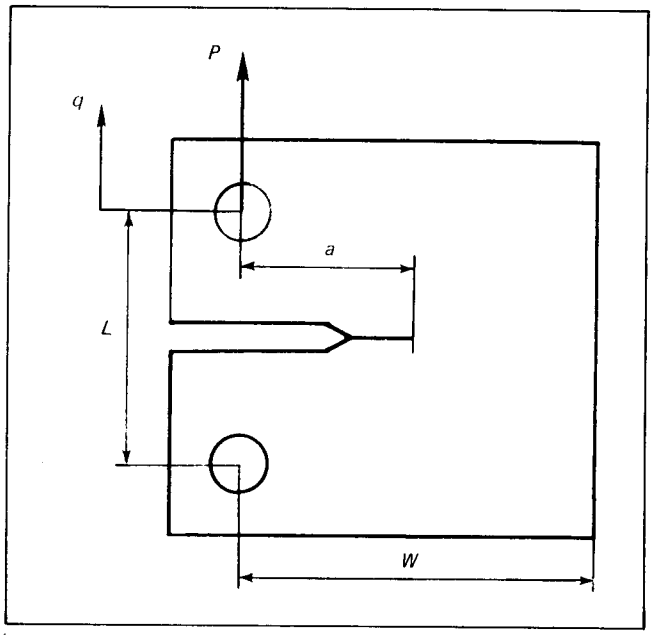

Fig. 10 Schematic illustration of compact tension test. Specimen thickness is *B*

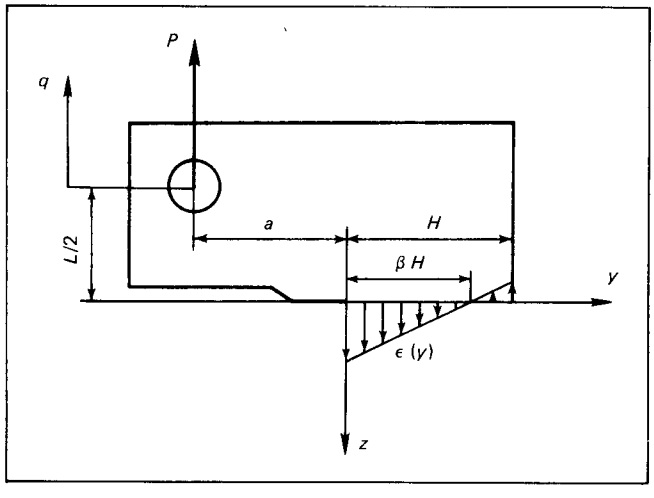

Fig. 11 Assumed strain field in CTS

of concrete matrix is generally an order of magnitude higher than its tensile strength.

The strain field shown in Fig. 11 can be expressed as:

$$\varepsilon(y) = \frac{\beta H - y}{\beta H + a}\left(\frac{q}{L}\right) \tag{19}$$

where β indicates the normalized position of the neutral plane, and *a*, *H*, and *L* are dimensions of the specimen. Force balance in the vertical direction requires:

$$P = \int_0^H B\,\sigma(\varepsilon)\,dy \tag{20}$$

and moment balance about a point on the loading line gives:

$$0 = \int_0^H B\,(a - y)\,\sigma(\varepsilon)\,dy \tag{21}$$

When the extended tensile stress–strain relation is used as σ(ε) in the above equations, β in Equation (19) can be found from Equation (21), and the the force *P* can be calculated for each displacement value (*q*) from Equation (20).

Flexural model

Similar to what was done for the CTS model, consider now a beam under pure bending moment (*M*) illustrated in Fig. 12. The curvature of the beam is measured by the mid-span displacement (f_c), which is related to the maximum tensile strain (ϵ_t) by:

$$f_c = \left(\frac{\beta H}{\varepsilon_t} + \beta H\right)\left(1 - \cos\frac{L\varepsilon_t}{2\beta H}\right) \tag{22}$$

The assumed linear strain field is given by:

$$\varepsilon(y) = \frac{\beta H - y}{\beta H}\,\varepsilon_t \tag{23}$$

From force equilibrium in *x*-direction:

$$0 = \int_0^H B\,\sigma(\varepsilon)\,dy \tag{24}$$

from which β, the normalized neutral plane location, is found. Moment balance requires:

$$M = \int_0^H B\,(\beta H - y)\,\sigma(\varepsilon)\,dy \tag{25}$$

When the extended tensile constitutive relation is used, the complete moment versus mid-span displacement relation can be calculated from these equations.

Experiments

Concrete matrix composed of cement (Type III), sand (#45 silica), and water (weight ratio cement:sand:water = 1:1:0.5) was reinforced with randomly distributed staple nylon and acrylic fibres of various geometries and tested in the CTS and flexural tests. Details on mixing, testing, and results have been reported elsewhere.[8,9]

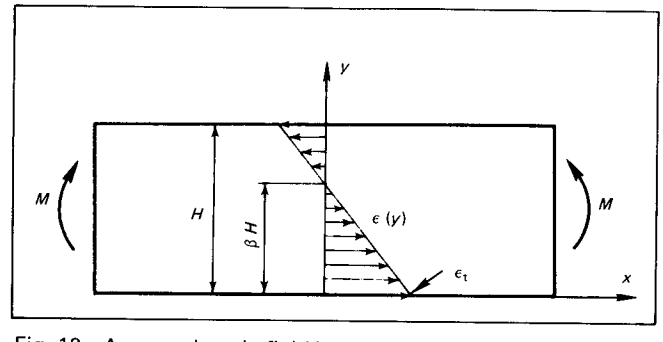

Fig. 12 Assumed strain field in a purely bent beam. Beam width is *B*

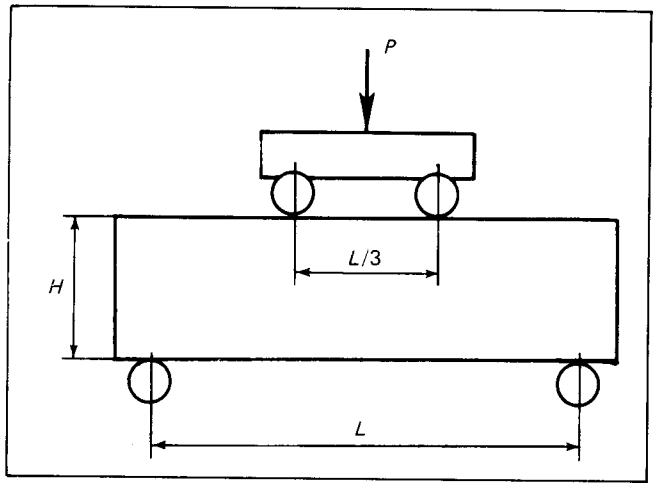

Fig. 13 Schematic diagram for the flexural test. Major span length L = 305 mm

In the CTS test, specimens were cut into the geometry shown in Fig. 10 with the following dimensions: W = 81.0 mm, L = 57.2 mm, B = 50.8 mm, and a = 38.1 mm. They were then tested on an Instron machine at a specimen age of about 50 days. The relation of load versus load line displacement measured at the crack mouth with a clip gauge was recorded for each test.

In the flexural test, cast beams of 102 × 102 × 356 mm were tested in four point bending, following the ACI guide for FRC flexural strength test.[11] A schematic diagram for the test set-up is shown in Fig. 13. The deflection was measured at the beam mid-span location. The specimen age at test was about 120 days.

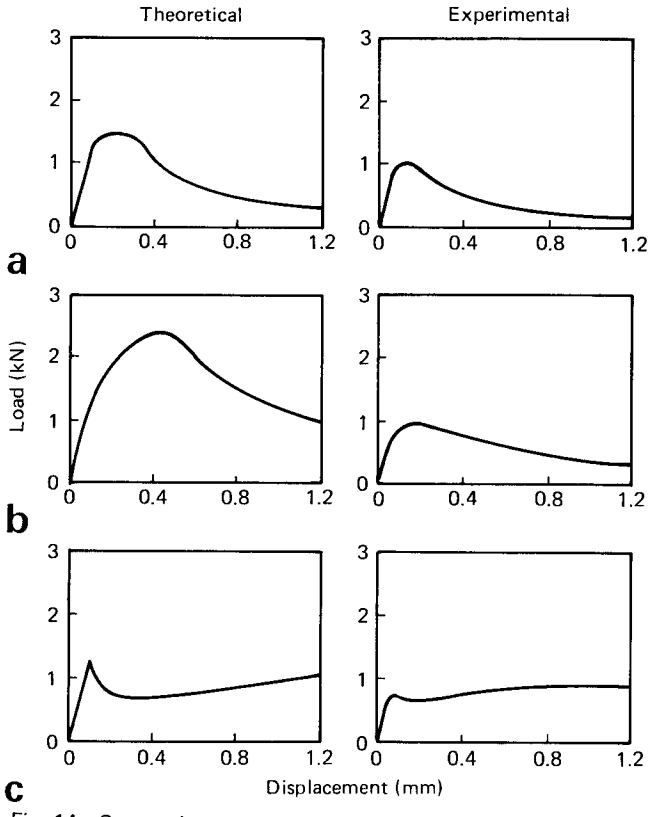

Fig. 14 Comparison of theoretical (left) and experimental (right) results for CTS tests. (a) Acrylic FRC: V_f = 2%, L_f = 12.7 mm, and d_f = 0.0136 mm; (b) acrylic FRC: V_f = 4%, L_f = 6.4 mm, and d_f = 0.0192 mm; (c) nylon FRC: V_f = 2%, L_f = 38.1 mm, and d_f = 0.0176 mm

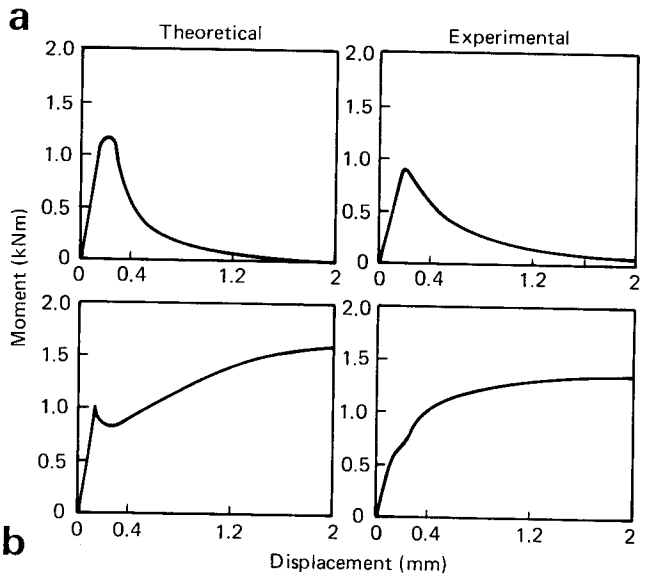

Fig. 15 Comparison of theoretical (left) and experimental (right) results for flexural tests. (a) Acrylic FRC: V_f = 2%, L_f = 19.1 mm, and d_f = 0.0192 mm; (b) nylon FRC: V_f = 2.4%, L_f = 38.1 mm, and d_f = 0.0176 mm

Comparisons of theoretical and experimental results

Comparisons of theoretical and experimental curves of load–displacement relations for the CTS test are provided in Fig. 14 for nylon FRC and for acrylic FRC with two different fibre volume fractions. Similar comparisons of nylon and acrylic FRC for the flexural test are given in Fig. 15.

From Figs 14 and 15, it can be seen that the load–deformation behaviour of FRC being considered varies significantly with different fibre reinforcements, and that the theoretical results agree well qualitatively with the experimental results in general. It is also interesting to note that due to the structural constraints of these test configurations, the tests are predicted to be stable (ie, no sudden load drops) at the instant of matrix cracking, and this was indeed observed in the experiments.

DISCUSSION AND CONCLUSIONS

A statistical model of the tensile constitutive relation of FRC was established based on the fibre distribution relative to the crack across the matrix of FRC. Although this model was developed for FRC, it may as well apply to other short fibre reinforced composites with brittle matrices. This model was also related to the load–displacement relations for CTS and flexural tests by two simplified models.

The theoretical results for the CTS and flexural test configurations were compared with experimental results of nylon and acrylic FRC. Good qualitative agreement between theory and experiment of FRC

behaviour was found, which indicates the usefulness of this model in studying FRC behaviour with respect to fibre and matrix properties and fibre volume fraction. This agreement also encourages further studies to improve the experimental techniques as well as to improve the model itself, in order to achieve quantitative agreement between theoretical and experimental results.

It is therefore helpful to identify the factors that might have contributed to this quantitative discrepancy in order to provide guidelines for further theoretical and experimental studies currently underway.

In this study, theoretical results were compared with experimental results from CTS and flexural tests through the use of simplified models which were based on assumed strain fields. In addition, the loading configuration for the flexural test (four point bending) differed in certain respects from the assumption of pure bending. Therefore it would be reasonable to partially attribute this discrepancy to the use of the CTS and flexural models. A well controlled uniaxial tension test of FRC should certainly provide more useful information about the FRC behaviour and thus allow direct verification of the theoretical model.

Examination of the crack surfaces of the specimens tested in the CTS and flexural tests revealed that the crack of the specimen formed a complex rough surface representing failure where the matrix or fibre/matrix interfaces were the weakest, rather than lying along a plane surface. Also the fibres in the matrix appeared in bundle form, rather than separated. The effect of fibre bundling is very complicated, as the presence of fibre bundles reduces the effective fibre volume fraction since the fibres in the middle of the bundle are not subjected to independent pull-out. Improvement in specimen fabricating techniques to achieve better homogeneity is an absolute necessity. In any event, modification of assumptions in the model to account for fibre bundles in the matrix is necessary.

Concrete shows inelastic deformation and strain softening in tension due to microcracking. For simplicity, this model assumed the matrix to be linear elastic up to cracking. Inaccuracy in the model's predictions was therefore expected for strains near that of matrix cracking.

Based on the theoretical as well as the experimental results, it was seen in some cases that the maximum loads could be higher than those at the instant of matrix cracking, indicating the possibility of multiple cracking of the FRC matrix. Therefore the single fracture assumption may be violated for some cases. In this study, due to the constraint of the test configurations and the inhomogeneity of the test specimens, multiple fractures were not observed in the CTS test, and seldom found in the flexural test. However, for FRC with better homogeneity or under special test conditions (uniaxial tension, for example), determination and consideration of multiple fractures should be an integral part of the theoretical modelling of FRC tensile behaviour.

The assumption of constant shear yield stress in the fibre/matrix bond along the fibre deserves, and is being paid more attention. A detailed study of the fibre/matrix interfacial bond will lead to a more realistic and more accurate characterization of the pull-out of fibres bridging the crack. Still another aspect of fibre-matrix interaction should be considered, particularly as related to the bending of a fibre which is inclined to the crack plane. The likelihood of fibre snubbing or plowing at the exit corner must be explored. Other assumptions in the model should also be reexamined and the possibilities of using specially designed fibres (eg, varying cross section along fibre) should be considered as well.

ACKNOWLEDGEMENTS

The early part of this research programme has been supported in part by the E. I. du Pont de Nemours & Co. Inc., for which we express our appreciation. We acknowledge funding from the Shimizu Construction Co. Ltd., Tokyo, and the National Science Foundation for the ongoing research programme.

REFERENCES

1 **Klos, H. G.** 'Properties and Testing of Asbestos Fibre Cement', In: *RILEM Symposium 1975: Fibre Reinforced Cement and Concrete*, Ed. A. Neville (Construction Press, Lancaster, 1975) pp 259–267

2 **Romualdi, J. P. and Batson, G. B.** 'Mechanics of Crack Arrest in Concrete', *Proceedings of ASCE*, Vol. 89, No. EM3 (1963) pp 147–168

3 **Argon, A. S. and Shack, W. J.** 'Theories of Fibre Cement and Fibre Concrete', in: *RILEM Symposium 1975: Fibre reinforced Cement and Concrete*, Ed. A. Neville (Construction Press, Lancaster, 1975) pp 39–53, 509–513

4 **Naaman, A. E.** 'A Statistical Theory of Strength for Fibre Reinforced Concrete', *PhD Thesis*, Department of Civil Engineering, Massachusetts Institute of Technology (1972)

5 **Aveston, J., Cooper, G. A. and Kelly, A.** 'Single and Multiple Fracture', in: *The Properties of Fibre Composites*, Conference Proceeding, National Physics Laboratory, (IPC Science and Technology Press, 1971) pp 15–26

6 **Ganeshalingham, R., Paramasivam, P. and Nathan, G. K.** 'An Evaluation of Theories and a Design Method of Fibre Cement Composites', *Int J Cement Composites Lightweight Concrete* **3,** No. 2 (1981) pp 103–114

7 **Li, V. C. and Liang, E.** 'Fracture Processes in Concrete and Fibre Reinforced Cementitious Composites', *ASCE J Eng Mech* **112** 6 (1986) pp 566–586

8 **Wang, Y.** 'Mechanics of Fibre Reinforced Concrete', *SM Thesis*, Department of Mechanical Engineering, Massachusetts Institute of Technology (1985)

9 **Wang, Y., Backer, S. and Li, V. C.** 'An Experimental Study of Synthetic Fibre Reinforced Cementitious Composites' *J Mater Sci* **22** (1987) pp 4281–4291

10 **Wang, Y., Backer, S. and Li, V. C.** 'A Special Technique for Determination of the Critical Length of Fibre Pull-out From a Cement Matrix' *J Mater Sci Lett* **7** (1988) pp 842–844

11 ACI Committee 544, 'Measurement of Properties of Fibre Reinforced Concrete', ACI 544.2R-78, *ACI Manual of Concrete Practice* (1986)

AUTHORS

Youjiang Wang and Stanley Backer are with the Department of Mechanical Engineering, and Victor C. Li is with the Department of Civil Engineering, Massachusetts Institute of Technology, Cambridge, Massachusetts 02139, USA. Enquiries should be addressed to Victor C. Li.